ACS OMEGA

Open Access

http://pubs.acs.org/journal/acsodf

Article

Sensing the Bactericidal and Bacteriostatic Antimicrobial Mode of Action Using Raman Deuterium Stable Isotope Probing (DSIP) in *Escherichia coli*

Jiro Karlo, Arunsree Vijay, Mahamkali Sri Phaneeswar, and Surya Pratap Singh*

Cite This: *ACS Omega* 2024, 9, 23753−23760

Read Online

ACCESS | Metrics & More | Article Recommendations | Supporting Information

ABSTRACT: The mode of action of antibiotics can be broadly classified as bacteriostatic and bactericidal. The bacteriostatic mode leads to the arrested growth of the cells, while the bacteriocidal mode causes cell death. In this work, we report the applicability of deuterium stable isotope probing (DSIP) in combination with Raman spectroscopy (Raman DSIP) for discriminating the mode of action of antibiotics at the community level. *Escherichia coli,* a well-known model microbe, was used as an organism for the study. We optimized the concentration of deuterium oxide required for metabolic activity monitoring without compromising the microbial growth. Our findings suggest that changes in the intensity of the C−D band in the high-wavenumber region could serve as a quantifiable marker for determining the antibiotic mode of action. This can be used for early identification of the antibiotic's mode of action. Our results explore the new perspective that supports the utility of deuterium-based vibrational tags in the field of clinical spectroscopy. Understanding the antibiotic's mode of action on bacterial cells in a short and objective manner can significantly enhance the clinical management abilities of infectious diseases and may also help in personalized antimicrobial therapy.

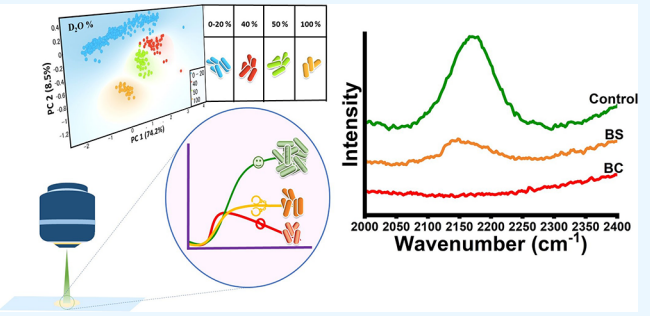

INTRODUCTION

The widespread usage of antibiotics without a prescription and contamination caused by antibiotic residues are pushing the world to the antimicrobial resistance-based serious public health issue.[1−4] The bactericidal and bacteriostatic efficacy of antibiotics plays a major role in guiding the treatment strategies for bacterial infections. Understanding the differences in the modes of action of antibiotics assists in identifying the right antibiotic. Bactericidal antibiotics operate by inducing microbial cell death. It may occur via disruption of the cellular structures, such as cell walls, and other important metabolic functions. In contrast, bacteriostatic antibiotics inhibit cell growth or division without causing immediate cell death. Having said that, bacteriostatic antibiotics also can kill bacteria at higher doses.[5] The mode of action of antibiotics is also concentration-dependent. Commonly used bactericidal antibiotics are fluoroquinolones and β-lactam, whereas bacteriostatic antibiotics are chloramphenicol, tetracyclines, trimethoprim/sulfamethoxazole, linezolid, macrolides, and clindamycin.[2,6] Despite their extensive antimicrobial activity, bacteriostatic antibiotics often inhibit the growth of microbes, thus they work synergistically with the host's immune system to get rid of the microbes.[2,6−8] Treating the patient with this class of antibiotics does not require intensive monitoring.[6,7] In our study, we have used different antibiotics, among which norfloxacin and ciprofloxacin are bactericidal (BC) in nature, while chloramphenicol and tetracycline are bacteriostatic (BS).[2,9] These antibiotics are used for the treatment of many infectious diseases; for example, norfloxacin is used to treat acute diarrhea, complicated urinary tract infections (UTIs), and gonococcal urethritis; ciprofloxacin is effective in treating UTIs, gall bladder infections, serious gastrointestinal infections, eye infections, gonorrhea; chloramphenicol is effective as conjunctivitis eyedrops, ointment for surgical wounds; tetracycline is used for the treatment of many bacterial infections including acne vulgaris.[10−15] This broad binary classification system of antibiotics varies in different organisms with corresponding concentrations.[9] In our study, we have used *Escherichia coli* to evaluate the efficacy of these antibiotics. *E. coli* are found in the gastrointestinal tract of humans and are rarely infectious unless the host immune system or barriers of the gastrointestinal area are compromised. However, some of

Received: February 21, 2024
Revised: May 10, 2024
Accepted: May 15, 2024
Published: May 22, 2024

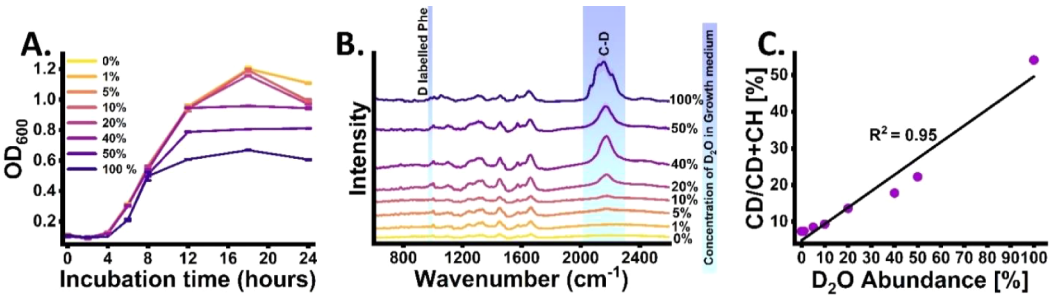

Figure 1. Identifying optimal deuterium concentration on *E. coli* cells. (A) Growth profile at different concentrations of D_2O in culture medium with incubation time points. (B) Average Raman spectra of *E. coli* cells cultured in different D_2O abundance. (C) Plot showing relation between ratiometric CD/CD+CH intensity percentage with D_2O abundance in the culture medium (shaded area shows the standard deviation).

the *E. coli* strains that are pathogenic cause infections, such as diarrhea, urinary tract infections, meningitis, and sepsis.[16]

The existing gold standard method to differentiate between bactericidal or bacteriostatic activity of antibiotics is through optical density measurements.[17] Another well-known technique is the kill experiment, which involves estimating the colony counts on agar plates measuring the microbial cell density.[9] In addition, visual inspection for determining the efficacy of antibiotics is performed using the disk diffusion method and spread plate method.[18] Even though these methods are highly reliable, early detection and biomolecular information cannot be achieved through these techniques. Furthermore, just detecting/identifying cells does not necessarily indicate that the cells are metabolically active or viable. Polymerase chain reaction-based antibiotic susceptibility tests are genotypic methods which are used for faster screening of resistance genes and are culture-free methods but are not suitable for classifying the efficacy of antibiotics on bacterial species.[19,20]

Deuterium oxide (D_2O) or heavy water is used as the source of the vibrational probe in the culture medium to substitute the hydrogen (^1H) atom with deuterium ($^2H/D$) in the cellular biomass. When D is substituted in the carbon−hydrogen (C−H) bond, it gives a unique prominent peak in the Raman silent region, which can act as the spectral metabolic activity marker. This also leads to the appearance of other unique biomolecular peaks.[21,22] The deuterium stable isotope probing methodology with heavy water as the probing source for the microbial study was introduced by Berry et al. for identifying and sorting active microbes.[23] The appearances of new deuterated peaks that are red-shifted arise due to the isotopic effect, i.e., the substitution of H by D leading to an increase in the reduced mass of the molecular bond owing to a decrease in wavenumber.[22,24,25] This C−H/D biomolecular substitution occurs due to the rapid intracellular biocatalytic exchange between D of D_2O and H atom of nicotinamide adenine dinucleotide phosphate (NADPH) which is redox active.[20,22] Previously, Bernatová et al. reported the use of Raman spectroscopy for investigating the action mechanism of bactericidal and bacteriostatic action based on DNA and protein signals in the Raman bio fingerprint region (600−-1800 cm^{-1}) of *Staphylococcus epidermis*.[2]

In this study, we propose an alternate combinatorial route based on the principles of Raman spectroscopy and deuterium isotope labeling for identifying the metabolic activity of bacterial strain *E. coli* under the influence of bacteriostatic and bacteriocidal activity of antibiotics. Understanding the mode of action of antibiotics can assist in the clinical management of infectious diseases by customizing the patient's antimicrobial therapy requirements. This method has the hidden potential for clinical translation for determining the nature and the concentration-dependent activity of antibiotics thereby reducing treatment time.

METHODOLOGY

Bacterial Growth and Treatment Conditions. The bacterial strain *Escherichia coli* was used. It was cultivated in a growth culture medium (M9 minimal medium − Sigma-Aldrich) agar plate and incubated at 37 °C. A single colony from the culture plate was inoculated in the broth medium and incubated at 37 °C and 120 rpm on the rotational shaker. From the overnight culture, reinoculation was done in the culture medium (M9 minimal medium − Sigma-Aldrich) with different concentrations of deuterium oxide (0%, 1%, 5%, 10%, 20%, 40%, 50%, and 100%). The growth profile was determined using OD_{600} value using Epoch 2 microplate spectrophotometer at different incubation time points at 0, 1, 2, 4, 8, 12, and 24 h (2×). Following the overnight culture, the culture medium was reinoculated with and without antibiotics. The working concentration of antibiotics used in the study was optimized by studying the growth curve, which included the static and kill curves, referring to the previous literature.[2,26,27] Antibiotics namely norfloxacin (Tokyo Chemical Industry), ciprofloxacin, tetracycline, and chloramphenicol (Sisco Research Laboratories) were used. The growth profile was determined by measuring the OD_{600} value with the aforementioned procedure.

Sample Preparation. To determine the optimal D_2O concentration, aliquots were taken at 18 h post inoculation from bacterial culture with different D_2O concentrations. The cells were centrifuged at 7000*g* for 5 min, and the pellets were washed twice with phosphate buffer saline (PBS, Sisco Research Laboratories) to remove the media traces. Cell pellets were mounted on an ethanol-washed CaF_2 window and air-dried. The washed cell pellets from an overnight culture were resuspended in the growth medium supplemented with 40% D_2O, with and without antibiotics. Post inoculation, the aliquots were collected at different time points such as 0, 1, 2, 4, 8, 12, and 24 h. Cell pellets were mounted on an ethanol-washed CaF_2 window and air-dried as per the procedure mentioned previously.

Raman Data Acquisition and Multivariate Analysis. For acquiring Raman spectra, WITec Confocal Raman Micro spectrometer alpha 300 access was used. The system had a 532 nm laser source and 100× objective with a 0.8 numerical aperture. Raman spectra were collected at different spots on the cell pellet and each spectrum was averaged over 10

https://doi.org/10.1021/acsomega.4c01666
ACS Omega 2024, 9, 23753−23760

accumulations with an exposure time of 10 s in the spectral range of 200 to 3200 cm^{-1}. The acquired spectral data were preprocessed using MATLAB R2021b software. The raw data were smoothened and Savitzky Golay filtered. It was baseline corrected with a third-order polynomial and unit normalized. The CD/CD+CH ratiometric percentage was calculated by taking the normalized integrated intensity of the carbon deuterium (2070−-2300 cm^{-1}) and carbon hydrogen (2800−3100 cm^{-1}) band in the high wavenumber region. The principal component analysis was performed in MATLAB R2021b software using preprocessed spectral data. All spectral plots and figures were generated using Origin Pro 2023b software, and the PCA score plot was generated using Orange software.

RESULTS AND DISCUSSION

Identifying Optimal Deuteration Level for Tracking Cellular Metabolic Activity. It has been well established in previously reported studies that the C−D band acts as a prominent Raman metabolic activity spectral marker for cells.[22,28−30] For validating the feasibility of the growth of *E. coli* in D_2O-labeled culture medium, microbial cells were grown in different concentrations at 0%, 1%, 5%, 10%, 20%, 40%, 50%, and 100%. Postinoculation, optical density measurements were performed at different time points; 0, 2, 4, 6, 8, 12, and 24 h. The growth curve is shown in Figure 1A. In the growth profile, the low abundance of D_2O concentration, with 1%, 5%, 10%, 20%, and 40% in the culture medium, had a similar pattern when compared to the growth profile of cells grown in control culture media (0% D_2O). However, with the increase in D_2O abundance from 50% to 100%, the corresponding growth profile also changes evidently. This retarded growth curve is probably due to toxicity at higher D_2O concentrations.

Hydrogen (H) bonds play an important role in the biomolecular structure, function, and interaction. Previously reported studies have reported that the substitution of H with D affects the hydrogen bond, disruption of OH/D group orientation and change in symmetry, lipid−protein interactions, protein denaturation process, and lipid bilayer.[22,30−32] At these concentrations, the stationary phase was found to be reached earlier, suggesting that a higher D_2O abundance has a negative effect on the growth of the microbial cells.

These observations provided evidence that the optimal concentration for microbial growth in the presence of D_2O should be in the range of 1% to 40%. However, this optimal concentration may vary in different strains. After analyzing the growth profile at different D_2O concentrations, the next step of the analysis was to determine the preferable D_2O percentage for ensuring a proper detectable signal intensity from the C−D Raman band. Post-inoculation, Raman spectra of the microbial cells were recorded at the 18 h time point at different D_2O percentages as shown in Figure 1B. In the cells growing with 0% deuteration, no visible C−D signal was observed in the high wavenumber region between 2070 and 2300 cm^{-1}. The evolution of the peak occurs with increasing deuteration levels. However, in cells growing in 20% of the deuteration source, the observed C−D peak had a lower intensity. A prominent C−D peak appeared in cells growing at a 20% or higher deuterium concentration. This new peak majorly arises due to the redshift of the C−H band between 2800 and 3100 cm^{-1} (Table 1). The red shift of the band occurs when protium is substituted by deuterium, which has a double mass. This increase in reduced mass leads to a decrease in vibrational frequency and the corresponding redshift toward a lower wavenumber.[22,25,28,29] In Figure 1B, with the increasing availability of D_2O abundance 0%, 1%, 5%, 10%, 20%, 40%, 50%, and 100%, the deuterium-substituted biomolecular Raman bands become prominent.

Table 1. Band Assignments of the Deuterated Biomolecules

unlabeled bands (cm^{-1})	D labeled bands (cm^{-1})	peak assignment	references
2800−3100	2070−2300	C−H/D	22,23,28,29,33
1003	989	phenylalanine	21,22

However, the C−D band intensity at 20% to 100% D_2O was more prominent when compared to the intensity at D_2O abundance ranges from 0% to 10%. The observed spectral pattern indicates *de novo* substitution of deuterium (H/D) from the culture medium to the cellular biomolecules. Further, we have also analyzed the biofingerprint region between 600 and 1800 cm^{-1} to analyze the deuteration rate with D_2O abundance. It has been previously reported that the deuterated phenylalanine, a protein Raman spectral marker, has peaks at 989 cm^{-1}. It is red-shifted from position at 1003 cm^{-1}.[21] These peaks were visible only in concentrations ranging from 20% to 100% deuteration level. The correlation plot between the ratiometric percentage of CD/CD+CH intensity versus the D_2O abundance shows an approximately linear increment relation with a 0.95 correlation coefficient (R^2) (Figure 1C).

Furthermore, to investigate the reproducibility and changes of the Raman spectra from the microbes incubated in increasing D_2O abundance using the biofingerprint region which has the deuterium-substituted biomolecular peaks in much lower intensity when compared to the C−D signal in the high wavenumber region, we performed multivariate analysis using principal component analysis (PCA) as shown in Figure 2. The scatter plot between principal components (PC) 1 and 2 shown in Figure 2A yielded distinct clusters for cells treated with a higher deuterium concentration. The clusters of 0 to 20% D_2O abundance were clustered in one group, whereas the clusters of 40%, 50%, and 100% clustered with minimal overlapping. The scree plot shown in Figure 2B demonstrated an elbow-shaped curve indicating maximum significant variance in the first two principal components which gives 82.7% of the overall variance, and the corresponding loading plot is shown in Figure 2C. The loading plot helps to determine and interpret the biochemical representation by each PC. Comparing the findings of Figures 1A,Band 2A, the 40% D_2O abundance seems to be the ideal concentration in order to assess significant C−D band intensity which is subjected to vary strain wise.

Bacteriostatic and Bactericidal Antibiotic Activity Using Optical Density Measurements. To monitor and demonstrate the variability in the antibiotic mode of action, *E. coli* was cultured with and without the antibiotics at 40% D_2O concentration. The growth kinetics profile through optical density (600 nm) measurement of different time points at 0, 1, 2, 4, 8, 12, and 24 h was explored (Figure 3A,B). Upon monitoring, the untreated microbial growth shows a conventional sigmoidal curve. The incubation time of 6 h was chosen for antibiotic treatment (marked) as the microbial culture at this time appeared to be in the logarithmic phase. In Figure 3A, the bacteriostatic antibiotic-treated growth curve is displayed where it can be observed that the early stationary phase is reached at 2 h post antibiotic treatment suggesting inhibited

https://doi.org/10.1021/acsomega.4c01666
ACS Omega 2024, 9, 23753−23760

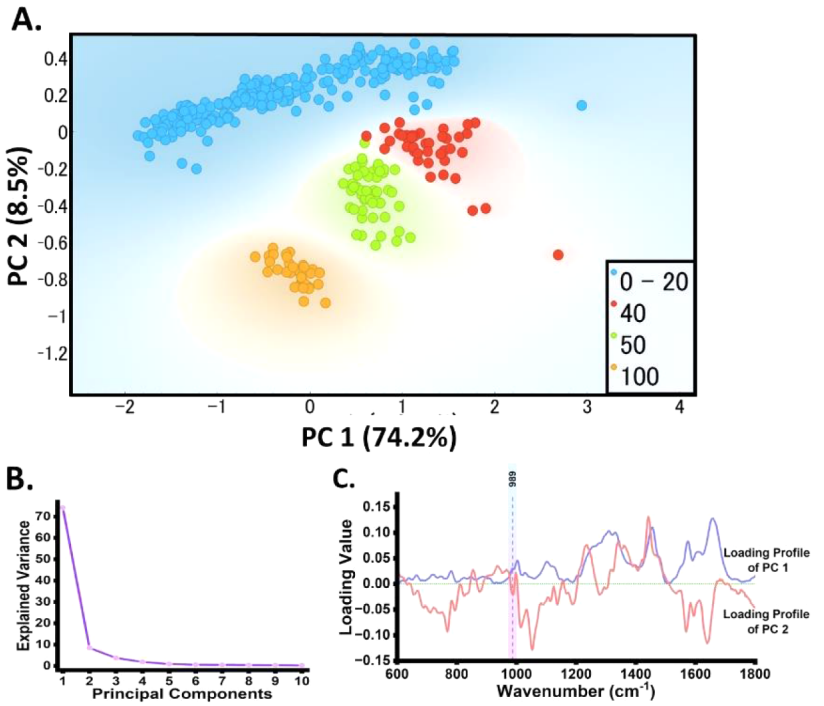

Figure 2. Discrmination of Raman spectra of deuterated *E. coli* (biofingerprint region) cells growing in different D_2O abundance using principal component analysis (PCA); (A) score plot between principal component 1 and principal component 2; (B) scree plot showing variance contributions by first 10 PCs; (C) loading profile of PC1 and PC2 in the biofingerprint region.

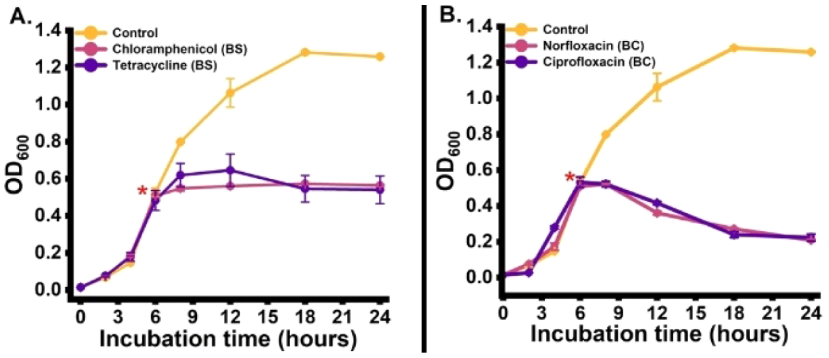

Figure 3. Growth profile of *E. coli* in culture medium with antibiotic treatment at 6 h; (A) bacteriostatic antibiotic activity (BS; chloramphenicol and tetracycline); (B) bactericidal antibiotics activity (BC; norfloxacin and ciprofloxacin). [* – Treatment time point].

growth of the microbial culture. In contrast, Figure 3B shows that the bacteria have been treated with bactericidal antibiotics and demonstrate a halt in the growth and decline of the growth curve with incubation time. This declining curve indicates the induction death phase in the culture medium.

Raman DSIP in the High Wavenumber Region Unravels the Bacteriostatic and Bactericidal Antibiotic Action. To investigate the action of bacteriostatic and bactericidal antibiotics on microbial activity using Raman DSIP, the microbial culture medium was prepared with the optimized 40% D_2O concentration. Before inoculation, the culture medium was treated with different aforementioned antibiotics, namely, chloramphenicol (30 μg mL^{-1}), tetracycline (12.5 μg mL^{-1}), norfloxacin (50 μg mL^{-1}), and ciprofloxacin (50 μg mL^{-1}). The working concentration of antibiotics with bacteriostatic and bactericidal activity was optimized by analyzing the static and kill curves of the bacterial growth profile as shown in Figure 3. Post-inoculation Raman spectra of the untreated and treated cells were recorded at different time points starting from 0, 1, 2, 4, 8, 12, and 24 h as shown in Figure 4. At 0 h, no detectable C−D peak in the region between 2030 and 2300 cm^{-1} was observed for both untreated and treated cells. At the early time points from 1 and 2 h, we observed a small C−D band in the Raman silent region from the untreated cells. Similarly, we also observed the emergence of the C−D band intensity from the growth-inhibited cells due to the bacteriostatic mode of action. In contrast, negligible C−D band intensity was observed from the cells under bactericidal antibiotic treatment. This qualitative difference in the C−D band intensity at early hours indicates the efficacy of this approach in tracking the differences in the mode of action of antibiotics. Further, with the increase in the incubation time, we observed an intense C−D band from the untreated cells, whereas negligible dynamic changes in the C−D band intensity was observed from cells treate with bacteriostatic or bacteriocidal antibiotics. No changes in the C−D band intensity from treated cells with bactericidal mode of action corroborates the known fact that cells enter into the

https://doi.org/10.1021/acsomega.4c01666
ACS Omega 2024, 9, 23753−23760

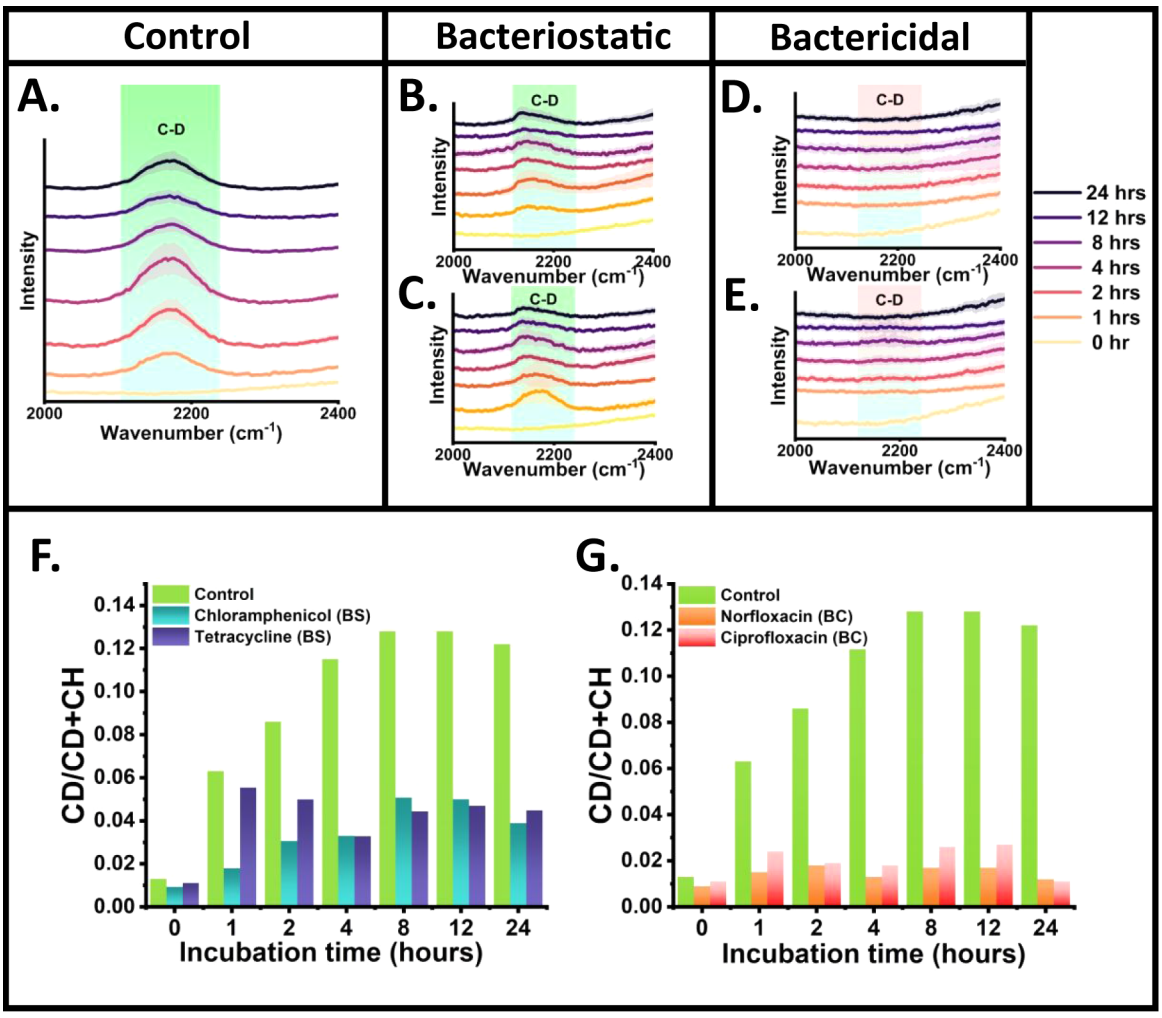

Figure 4. Raman deuterium stable isotope probing for differentiating the antimicrobial mode of action; qualitative analysis using Raman spectra of microbial cells in Raman silent reigion at different incubation time points. (A) Control, (B) chloramphenicol treated, (C) tetracycline treated, (D) norfloxacin treated, (E) ciprofloxacin treated; quasi-quantitative analysis using relative ratiometric intensity (CD/CD+CH) with incubation time; (F) control cells versus bacteriostatic effected cells; (G) control versus bactericidal effected cells (shaded area shows the standard deviation).

death phase. For the quantification, we have calculated the band intensity ratio of C−D/C−D+C−H at different incubation time points for the treated and untreated cells as shown in Figure 4F,G. The relative ratiometric intensity difference between control and antibiotic-treated cells demonstrated a clear difference with an increase in incubation time. The CD/CD+CH ratio can reveal the dynamics of the newly synthesized C−D band value due to deuterium incorporation, with respect to the total carbon hydrogen pool in the cell. Further, we also determined the statistical significance between the C−D band intensity of the control and treated groups by performing a *t* test using Origin software as shown in Figure S1.

Raman DSIP in the Biofingerprint Region to Unravel the Differences in Antibiotic Mode of Action. The next analysis was to examine whether the D_2O incorporation also induces spectral changes in the biofingerprint region, which can be utilized as a metabolic marker to differentiate among different modes of antibiotic action. A weak peak observed at 989 cm^{-1} appears due to the deuteration of the microbial phenylalanine aromatic ring.[21,24,30] Another interpretation of origin of this band is due to the deuteration of scissoring CH_2 leading to the formation of CD_2.[30] As the deuterium concentration is at 40%, complete redshift of this band was not observed. This leads to a visible but weak signal at 989 cm^{-1}, which might act as a possible qualitative marker band for monitoring the deuteration level and corresponding metabolic activity. In Figure 5, in the Raman spectra of control and treated groups at the 989 cm^{-1} position, we observed no bands at 0 h postincubation. However, this peak appears at 1 h postincubation for the control group as shown in Figure 5A. This peak intensity suggests a metabolically active state of cells. In Figure 5B,C Raman spectra for the treated group show a lower intensity of 989 cm^{-1} at 1 h, which becomes weaker with time indicating the bacteriostatic mode of action on the cells. Moreover, in Figure 5D,E Raman spectra for the treated group showed negligible peak intensity changes at all incubation times, indicating the bactericidal mode of action on the cells.

Rapid understanding of the bacteriostatic and bactericidal activity of antibiotics can help clinicians to plan appropriate strategies for treatment of infectious diseases. Antibiotics can be used in accordance with the severity of the infection and host immune response. As a result, resistance develops spontaneously with potential side effects. In our work, we have used the Raman DSIP as a novel assay to rapidly analyze the mode of action of antibiotics. The differences between

https://doi.org/10.1021/acsomega.4c01666
ACS Omega 2024, 9, 23753−23760

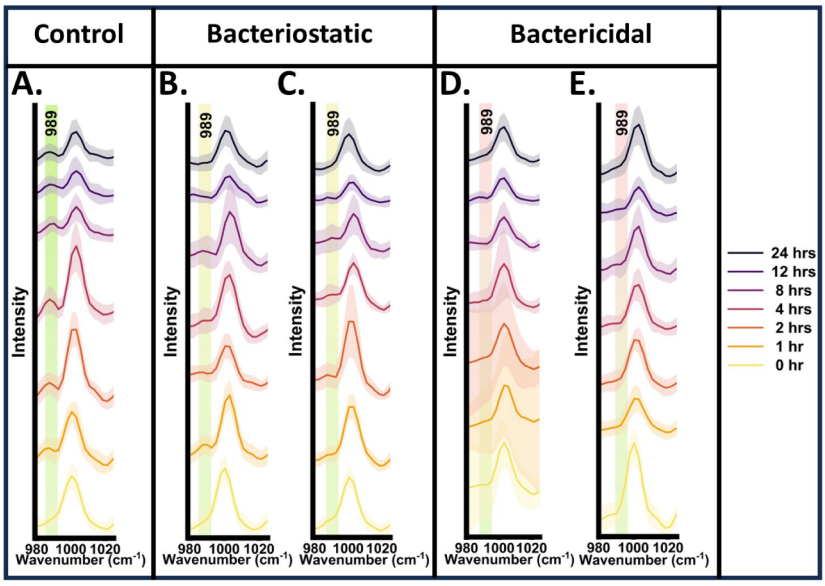

Figure 5. Deuterated band at 989 cm^{-1} in biofingerprint region as possible qualitative spectral marker band for differentiating the antimicrobial mode of action; qualitative analysis using average Raman spectra of microbial cells at biofingerprint region at different incubation time points. (A) Control (B) chloramphenicol treated, (C) tetracycline treated, (D) norfloxacin treated, (E) ciprofloxacin treated (shaded area shows the standard deviation).

bactericidal and bacteriostatic modes of action can be observed via the metabolic activity leading to a difference in C−D peak intensity. Raman spectroscopy is a nondestructive and noninvasive analytical technique with hidden potentials, which require further exploration by combining other methodologies such as stable isotope probing.[24,34] Recently, the Raman DSIP-based approach has been utilized to detect antimicrobial-resistant microbial species. Yang et al. showed the integration of Raman DSIP with advanced multivariate analysis to study the spectral dynamics to classify sensitive, intrinsic tolerant, evolved tolerant, and resistant cells.[35] Zhang et al. reported stimulated Raman DSIP and imaging-based strategy to detect metabolic incorporation of D_2O at single cell level and a rapid antimicrobial susceptibility test (AST) platform in a brief span of time of 10 min, which is claimed to be the fastest among currently available technologies.[20] Yi et al. developed a fast Raman-assisted antibiotic susceptibility test (FRAST) based on Raman DSIP for monitoring the metabolic activity of bacterial cells (Gram-negative and Gram-positive) in the presence of antibiotics.[36] Bauer et al. described a Raman DSIP-based AST protocol for Gram-positive/negative bacteria to detect heteroresistance phenotype and further conducted a proof of concept study by investigating the clinical isolates.[37] Xiao et al. reported an AST method based on Raman DSIP to explore the efficacy of last resort antibiotics (tigecycline, polymyxin B and vancomycin) against *Escherichia coli*, *Klebsiella pneumoniae*, *Pseudomonas aeruginosa*, and *Enterococcus faecium*.[38] Many other recent studies have explored the applicability and potential of the Raman DSIP approach for microbial metabolic activity and antimicrobial studies.[39−42] Although multiple studies have utilized D_2O concentration from 40% to 70%, we first optimized the feasible concentration which is necessary for the best survival of the microbe keeping a detectable C−D band under consideration. One of the remarkable findings of this study was to analyze the deuteration effect in the biofingerprint region and apply the multivariate analysis using PCA with classified clusters showing the difference in the percentage of deuteration in cells. Further, the bacteriostatic and bactericidal effect on cells was observed using spontaneous Raman scattering at a very early incubation time point. Though Raman DSIP is a highly feasible nondestructive approach, the D_2O has a toxic effect on the cells which we have shown and is the limitation in our study. The future perspective of the Raman DSIP approach lies in tracing the metabolic activity by increasing the C−D band detection sensitivity at very low concentrations of D_2O and in a short span of incubation time. This will minimize the toxic effect on the microbial metabolome and will promote Raman DSIP as a cost-effective approach to develop into a translational clinical assay for antimicrobial studies.

CONCLUSION

Our results suggest the dynamic changes in the intensity of the carbon−deuterium band in the Raman silent zone of the high wavenumber region can differentiate between the metabolic active, growth-arrested, and killed microbes. Further, we explored the possible potential of the deuterated biomolecular band in the biofingerprint region as a metabolic spectral marker for qualitative analysis of our mentioned goal. This work projects Raman DSIP as a prospective alternate biosensing assay to determine the efficacy of antibiotics and their concentration on the microbes at the community level. With this approach, the effect of antibiotics can be determined at early incubation time points. As the proposed method is efficient and simple, it holds immense potential for clinical translation as a tool for rapid classification of the antibiotics and concentration-dependent effects as bactericidal or bacteriostatic. The exploration of Raman DSIP holds the potential to be translated into a rapid clinical assay for the selection of appropriate antibiotics to treat infectious diseases and the detection of antimicrobial resistance and microbial dormancy.

https://doi.org/10.1021/acsomega.4c01666
ACS Omega 2024, 9, 23753−23760

■ ASSOCIATED CONTENT

Supporting Information

The Supporting Information is available free of charge at https://pubs.acs.org/doi/10.1021/acsomega.4c01666.

Plot of relative intensity changes in the C−D band from bacterial cells treated with bactericidal and bacteriostatic antibiotics at different time points (PDF)

■ AUTHOR INFORMATION

Corresponding Author

Surya Pratap Singh − *Department of Biosciences and Bioengineering, Indian Institute of Technology Dharwad, Dharwad, Karnataka 580011, India;* orcid.org/0000-0001-9984-5385; Email: ssingh@iitdh.ac.in

Authors

Jiro Karlo − *Department of Biosciences and Bioengineering, Indian Institute of Technology Dharwad, Dharwad, Karnataka 580011, India*

Arunsree Vijay − *Department of Biosciences and Bioengineering, Indian Institute of Technology Dharwad, Dharwad, Karnataka 580011, India*

Mahamkali Sri Phaneeswar − *Department of Biosciences and Bioengineering, Indian Institute of Technology Dharwad, Dharwad, Karnataka 580011, India*

Complete contact information is available at: https://pubs.acs.org/10.1021/acsomega.4c01666

Notes

The authors declare no competing financial interest.

■ ACKNOWLEDGMENTS

This work was carried out under research grant project no (37/1739/23/EMR-II) supported by the Council of Scientific and Industrial Research (CSIR), Government of India and project no. IIRP-2023-1734 from Indian Council of Medical Research (ICMR), Government of India.

■ REFERENCES

(1) Wintenberger, C.; Guery, B.; Bonnet, E.; Castan, B.; Cohen, R.; Diamantis, S.; Lesprit, P.; Maulin, L.; Péan, Y.; Peju, E.; et al. Proposal for Shorter Antibiotic Therapies. *Med. Mal. Infect.* **2017**, *47* (2), 92−141.

(2) Bernatová, S.; Samek, O.; Pilát, Z.; Šerý, M.; Jěek, J.; Jákl, P.; ̌iler, M.; Krzyánek, V.; Zemánek, P.; Holá, V.; et al. Following the Mechanisms of Bacteriostatic versus Bactericidal Action Using Raman Spectroscopy. *Molecules* **2013**, *18* (11), 13188−13199.

(3) Radlinski, L.; Conlon, B. P. Antibiotic Efficacy in the Complex Infection Environment. *Curr. Opin. Microbiol.* **2018**, *42*, 19−24.

(4) Novikov, A.; Sayfutdinova, A.; Botchkova, E.; Kopitsyn, D.; Fakhrullin, R. Antibiotic Susceptibility Testing with Raman Biosensing. *Antibiotics* **2022**, *11*, 1812.

(5) Wald-Dickler, N.; Holtom, P.; Spellberg, B. Busting the Myth of "Static vs Cidal": A Systemic Literature Review. *Clin. Infect. Dis.* **2018**, *66* (9), 1470−1474.

(6) Loree, J.; Lappin, S. L. *Bacteriostatic Antibiotics*; StatPearls Publishing: Treasure Island, FL, 2023.

(7) Vicente, D.; Pérez-Trallero, E. Tetraciclinas, Sulfamidas y Metronidazol. *Enferm. Infect. Microbiol. Clin.* **2010**, *28* (2), 122−130.

(8) Cobos-Trigueros, N.; Ateka, O.; Pitart, C.; Vila, J. Macrólidos y Cetólidos. *Enferm. Infect. Microbiol. Clin.* **2009**, *27* (7), 412−418.

(9) Ocampo, P. S.; Lázár, V.; Papp, B.; Arnoldini, M.; Abel zur Wiesch, P.; Busa-Fekete, R.; Fekete, G.; Pál, C.; Ackermann, M.; Bonhoeffer, S. Antagonism between Bacteriostatic and Bactericidal Antibiotics Is Prevalent. *Antimicrob. Agents Chemother.* **2014**, *58* (8), 4573−4582.

(10) Norrby, S. R. Norfloxacin: Targeted Antibiotic Therapy: Proceedings of a Workshop Held in Taormina, Sicily 11 April, 1986. *Scand J. Infect. Dis.* **1986**, *18* (sup48), 1−91.

(11) Rowen, R. C.; Michel, D. J.; Thompson, J. C. Norfloxacin: Clinical Pharmacology and Clinical Use. *Pharmacotherapy* **1987**, *7* (4), 92−106.

(12) Finch, R. G. Ciprofloxacin: Efficacy and Indications. *J. Chemother.* **2000**, *12* (sup1), 5−7.

(13) Cave, J. A. Chloramphenicol Eye Drops, Boron, Infants and Fertility. *Drug Ther. Bull.* **2021**, *59* (7), 98−98.

(14) Shen, A. Y.; Haddad, E. J.; Hunter-Smith, D. J.; Rozen, W. M. Efficacy and Adverse Effects of Topical Chloramphenicol Ointment Use for Surgical Wounds: A Systematic Review. *ANZ. J. Surg.* **2018**, *88* (12), 1243−1246.

(15) Rusu, A.; Buta, E. L. The Development of Third-Generation Tetracycline Antibiotics and New Perspectives. *Pharmaceutics* **2021**, *13* (12), 2085.

(16) Kaper, J. B.; Nataro, J. P.; Mobley, H. L. T. Pathogenic *Escherichia Coli*. *Nat. Rev. Microbiol.* **2004**, *2* (2), 123−140.

(17) Pedreira, A.; Vázquez, J. A.; García, M. R. Kinetics of Bacterial Adaptation, Growth, and Death at Didecyldimethylammonium Chloride Sub-MIC Concentrations. *Front. Microbiol.* **2022**, *13*, 758237.

(18) Gajic, I.; Kabic, J.; Kekic, D.; Jovicevic, M.; Milenkovic, M.; Mitic Culafic, D.; Trudic, A.; Ranin, L.; Opavski, N. Antimicrobial Susceptibility Testing: A Comprehensive Review of Currently Used Methods. *Antibiotics* **2022**, *11* (4), 427.

(19) Frickmann, H.; Masanta, W. O.; Zautner, A. E. Emerging Rapid Resistance Testing Methods for Clinical Microbiology Laboratories and Their Potential Impact on Patient Management. *BioMed. Res. Int.* **2014**, *2014*, 1−19.

(20) Zhang, M.; Hong, W.; Abutaleb, N. S.; Li, J.; Dong, P.; Zong, C.; Wang, P.; Seleem, M. N.; Cheng, J. Rapid Determination of Antimicrobial Susceptibility by Stimulated Raman Scattering Imaging of D_2O Metabolic Incorporation in a Single Bacterium. *Adv. Sci.* **2020**, *7*, 2001452.

(21) Wang, Y.; Song, Y.; Tao, Y.; Muhamadali, H.; Goodacre, R.; Zhou, N.-Y.; Preston, G. M.; Xu, J.; Huang, W. E. Reverse and Multiple Stable Isotope Probing to Study Bacterial Metabolism and Interactions at the Single Cell Level. *Anal. Chem.* **2016**, *88* (19), 9443−9450.

(22) Karlo, J.; Dhillon, A. K.; Siddhanta, S.; Singh, S. P. Reverse Stable Isotope Labelling with Raman Spectroscopy for Microbial Proteomics. *J. Biophotonics* **2023**, *17* (2), No. e202300341.

(23) Berry, D.; Mader, E.; Lee, T. K.; Woebken, D.; Wang, Y.; Zhu, D.; Palatinszky, M.; Schintlmeister, A.; Schmid, M. C.; Hanson, B. T.; et al. Tracking Heavy Water (D2O) Incorporation for Identifying and Sorting Active Microbial Cells. *Proc. Natl. Acad. Sci. U. S. A.* **2015**, *112* (2), No. E194−203.

(24) Karlo, J.; Gupta, A.; Singh, S. P. In Situ Monitoring of the Shikimate Pathway: A Combinatorial Approach of Raman Reverse Stable Isotope Probing and Hyperspectral Imaging. *Analyst* **2024**, *149* (10), 2833−2841.

(25) Karlo, J.; Dhillon, A. K.; Siddhanta, S.; Singh, S. P. Monitoring of Microbial Proteome Dynamics Using Raman Stable Isotope Probing. *J. Biophotonics* **2023**, *16* (4), No. e202200341.

(26) Lobritz, M. A.; Belenky, P.; Porter, C. B. M.; Gutierrez, A.; Yang, J. H.; Schwarz, E. G.; Dwyer, D. J.; Khalil, A. S.; Collins, J. J. Antibiotic Efficacy Is Linked to Bacterial Cellular Respiration. *Proc. Natl. Acad. Sci. U. S. A.* **2015**, *112* (27), 8173−8180.

(27) Santos, E. L.; Freitas, P. R.; Araújo, A. C. J.; Almeida, R. S.; Tintino, S. R.; Paulo, C. L. R.; Ribeiro-Filho, J.; Silva, A. C. A.; Silva, L. E.; Amaral, W. D.; et al. Phytochemical Characterization and Antibiotic Potentiating Effects of the Essential Oil of Aloysia Gratissima (Gillies & Hook.) and Beta-Caryophyllene. *S. Afr. J. Bot.* **2021**, *143*, 1−6.

(28) Xu, J.; Zhu, D.; Ibrahim, A. D.; Allen, C. C. R.; Gibson, C. M.; Fowler, P. W.; Song, Y.; Huang, W. E. Raman Deuterium Isotope Probing Reveals Microbial Metabolism at the Single-Cell Level. *Anal. Chem.* **2017**, *89* (24), 13305−13312.
(29) Yuan, S.; Chen, Y.; Lin, K.; Zou, L.; Lu, X.; He, N.; Liu, R.; Zhang, S.; Shen, D.; Song, Z.; et al. Single Cell Raman Spectroscopy Deuterium Isotope Probing for Rapid Antimicrobial Susceptibility Test of Elizabethkingia Spp. *Front. Microbiol.* **2022**, *13*, 876925.
(30) Omelchenko, A. N.; Okotrub, K. A.; Surovtsev, N. V. Raman Spectroscopy of Yeast Cells Cultured on a Deuterated Substrate. *Spectrochim. Acta, Part A* **2023**, *303*, 123262.
(31) Chen, C.-H. Deuterium Oxide and Deuteration Effects on Biomolecules. In *Deuterium Oxide and Deuteration in Biosciences*; Springer International Publishing: Cham, 2022; pp. 5971. .
(32) Shi, C.; Zhang, X.; Yu, C.-H.; Yao, Y.-F.; Zhang, W. Geometric Isotope Effect of Deuteration in a Hydrogen-Bonded Host−Guest Crystal. *Nat. Commun.* **2018**, *9* (1), 481.
(33) Jayan, H.; Pu, H.; Sun, D.-W. Analyzing Macromolecular Composition of *E. Coli* O157: H7 Using Raman-Stable Isotope Probing. *Spectrochim. Acta, Part A* **2022**, *276*, 121217.
(34) Karlo, J.; Prasad, R.; Singh, S. P. Biophotonics in Food Technology: Quo Vadis? *J. Agric. Food Res.* **2023**, *11*, 100482.
(35) Yang, K.; Xu, F.; Zhu, L.; Li, H.; Sun, Q.; Yan, A.; Ren, B.; Zhu, Y.; Cui, L. An Isotope-Labeled Single-Cell Raman Spectroscopy Approach for Tracking the Physiological Evolution Trajectory of Bacteria toward Antibiotic Resistance. *Angew. Chem., Int. Ed.* **2023**, *62* (14), No. e202217412.
(36) Yi, X.; Song, Y.; Xu, X.; Peng, D.; Wang, J.; Qie, X.; Lin, K.; Yu, M.; Ge, M.; Wang, Y.; et al. Development of a Fast Raman-Assisted Antibiotic Susceptibility Test (FRAST) for the Antibiotic Resistance Analysis of Clinical Urine and Blood Samples. *Anal. Chem.* **2021**, *93* (12), 5098−5106.
(37) Bauer, D.; Wieland, K.; Qiu, L.; Neumann-Cip, A.-C.; Magistro, G.; Stief, C.; Wieser, A.; Haisch, C. Heteroresistant Bacteria Detected by an Extended Raman-Based Antibiotic Susceptibility Test. *Anal. Chem.* **2020**, *92* (13), 8722−8731.
(38) Xiao, Z.; Qu, L.; Chen, H.; Liu, W.; Zhan, Y.; Ling, J.; Shen, H.; Yang, L.; Chen, D. Raman-Based Antimicrobial Susceptibility Testing on Antibiotics of Last Resort. *Infect. Drug. Resist.* **2023**, *16*, 5485−5500.
(39) Song, Y.; Cui, L.; López, J. Á. S.; Xu, J.; Zhu, Y.-G.; Thompson, I. P.; Huang, W. E. Raman-Deuterium Isotope Probing for in-Situ Identification of Antimicrobial Resistant Bacteria in Thames River. *Sci. Rep.* **2017**, *7* (1), 16648.
(40) Yuan, S.; Chen, Y.; Lin, K.; Zou, L.; Lu, X.; He, N.; Liu, R.; Zhang, S.; Shen, D.; Song, Z.; et al. Single Cell Raman Spectroscopy Deuterium Isotope Probing for Rapid Antimicrobial Susceptibility Test of *Elizabethkingia Spp*. *Front. Microbiol.* **2022**, *13*, 876925.
(41) Trigueros, S.; Brauge, T.; Dedole, T.; Debuiche, S.; Rebuffel, V.; Morales, S.; Marcoux, P. R.; Midelet, G. Deuterium Isotope Probing (DIP) on Listeria Innocua: Optimisation of Labelling and Impact on Viability State. *PLoS One* **2023**, *18* (3), No. e0280885.
(42) Azemtsop Matanfack, G.; Taubert, M.; Reilly-Schott, V.; Küsel, K.; Rösch, P.; Popp, J. Phenotypic Differentiation of Autotrophic and Heterotrophic Bacterial Cells Using Raman-D $_2$ O Labeling. *Anal. Chem.* **2022**, *94* (22), 7759−7766.

https://doi.org/10.1021/acsomega.4c01666
ACS Omega 2024, 9, 23753−23760